Multifrequency terahertz-wave emission and detection with the photomixing approach: theory and experiments

Florin Lucian Constantin

Multifrequency terahertz-wave emission and detection with the photomixing approach : theory and experiments

F. L. Constantin*[a]
[a]Laboratoire PhLAM, CNRS UMR 8523, 59655 Villeneuve d'Ascq, France

ABSTRACT

This contribution addresses theoretically and experimentally the photomixing signal in a low-temperature-grown GaAs (LTG-GaAs) device with a planar antenna that is driven with an alternative electric field superposed on a bias electric field. The total electric field is applied on the optically-driven nonlinear photoconductance of LTG-GaAs. A theoretical framework based on unidimensional carrier transport is developed to calculate the amplitudes and the phases of different spectral components of the current density. Radiofrequency modulation of the photomixing signal in the microwave domain is experimentally demonstrated. Conversely, the photomixer is exploited as an optically-driven detector. Heterodyne detection with a photomixer is experimentally demonstrated with modulated THz-waves. The photomixing approach allows to extract THz modulation parameters by measurements with a modulated optical beat.

Keywords: low-temperature-grown GaAs photomixer, optical frequency down-conversion, THz frequency comb, THz-wave modulation, THz-wave direct detection, THz-wave heterodyne detection

1. INTRODUCTION

The terahertz-waves are interesting for several applications including high-speed communications, spectroscopy, metrology and medical research[1]. Research in THz photonics has been driven by THz time-domain spectroscopy approach (THz-TDS)[2]. This approach has a problem of spectral resolution and requires massive femtosecond laser oscillators leading to a high system cost. The optical frequency conversion with a photomixer was developed for compact and cost-effective continuous-wave (cw) THz generation[3]. Two cw lasers emitting at frequencies f_1 and f_2 are mixed in an ultrafast photodetector with quadratic response to the optical fields. The photocurrent, oscillating at the frequency of the optical beat $f_{THz}=|f_1-f_2|$ in the terahertz domain, drives an antenna to generate monochromatic THz waves. The approach has the advantage to provide narrow spectral linewidth, wide frequency tunability, high dynamic range and high signal-to-noise ratio. The photomixer has been used as transmission element for high-speed communications that reached data rates higher than 100 Gbit/s [4]. In addition, the photomixing approach may provide system integration in compact setups using the silicon photonics technology[5].

This contribution addresses the generation and the detection of terahertz frequency combs with a photomixer based on low-temperature-grown GaAs photoconductor coupled to a planar antenna and driven by the optical beat of two continuous-wave lasers. A photomixing signal is generated by applying on the photoconductor an alternative electric field superposed on a bias electric field. The current density in the photomixer, driven by the optical beat, is expressed with carrier lifetimes and velocities that depend nonlinearily on the electric field applied to the photoconductor. A theoretical framework based on unidimensional carrier transport is developed to calculate the amplitudes and the phases of different spectral components of the current density. Bifrequency optoelectronic signal generation is addressed with a photomixer operated with an alternative voltage around zero-bias. Conversely, the photomixer is exploited as a detector for an electric field induced in the photoconductor by THz-waves. The resultant THz electric field is applied on the optically-driven nonlinear photoconductance, leading to rectification and THz-to-MW conversion that are theoretically and experimentally addressed[6]. In addition, THz waveforms are generated by modulation of a microwave synthesizer that drives a frequency multiplier. The heterodyne detection enables phase-sensitive detection of waveforms generated by frequency modulation.

*fl.constantin@univ-lille1.fr

2. PHOTOMIXING SIGNAL THEORY

Frequency mixing is addressed here with a model of unidimensional uniform carrier transport driven by various electric fields applied on the photoconductor. The continuity equations allow to express the total current density :

$$j(t)=\frac{2e\eta P}{\hbar\varpi Ad}\left[\tau_n v_n\left(1+\frac{\omega\tau_n\, sin(\omega t)+cos(\omega t)}{1+(\omega\tau_n)^2}\right)+\tau_p v_p\left(1+\frac{\omega\tau_p\, sin(\omega t)+cos(\omega t)}{1+(\omega\tau_p)^2}\right)\right] \quad (1)$$

where two laser beams with power P, energy $\hbar\varpi$, are used to make an optical beat at the angular frequency ω focused on a photoconductive area A with an absorption depth d with a quantum efficiency η. The carrier lifetimes $\tau_{n,p}$ have a nonlinear dependence with the electric field[7]. The last term adds small dependence on the electric field, and here a linear dependence on the total electric field E is considered:

$$\tau_{n,p}(E)\approx\tau_{0n,0p}[1+3\lambda eE/(2k_BT)] \quad (2)$$

where k_B is the Boltzmann constant, e electron charge, T=300 K is the room temperature, $\tau_{0n,0p}$ are the low-field carrier lifetimes and λ is the distance between Coulomb barriers in LTG-GaAs. The carrier drift velocities have a nonlinear dependence on the electrical field[8], which is expressed as :

$$v_{n,p}(E)=v_{sn,sp}/[1+v_{sn,sp}/(\mu_{0n,0p}E)] \quad (3)$$

where $v_{sn,sp}$ are the saturation velocities and $\mu_{0n,0p}$ are the low-field mobilities for electrons and holes.

Table 1. Experimental parameters for a LTG-GaAs photomixer

Photoconductor absorption depth d	2 μm	Low-field hole lifetime[8] τ_{0n}	0.4 ps
Photoconductor width r	2 μm	Low-field electron mobility[8] μ_{0n}	400 cm^2/Vs
Laser power P	10 mW	Low-field hole mobility[9] μ_{0p}	100 cm^2/Vs
Photoconductive area A	12.56 μm^2	Optical phonon mean free path[7] λ	7 nm
Laser frequency ν	365.85 THz	Distance between Coulomb barriers[7] a	2 nm
Electron saturation velocity[8] v_{sn}	40000 m/s	Dielectric constant ε	12.8
Hole saturation velocity[8] v_{sp}	10000 m/s	Antenna resistance R_A	72 Ω
Low-field electron lifetime[8] τ_{0n}	0.1 ps	Photomixer capacitance C	0.5 fF

An oscillating electric field can be applied to the photoconductor by coupling a radiofrequency (amplitude V_{RF}, angular frequency ω_{RF}) to the electrodes of the antenna. Alternatively, focusing a THz-wave on the antenna induces an equivalent Thévenin voltage on electrodes of the antenna which is expressed in the parallel-plate approximation in terms of the incident THz-electric field (amplitude $\vec{E}_{THz}^{inc}$, angular frequency ω_{THz}, phase φ_{THz}), the effective vector length $\vec{l}_{eff}$ of the antenna and the width of the photoconductive gap r. The total electric field inside the photoconductor can be expressed generally as alternative electric fields superposed to a bias electric field E_0:

$$E(t)=E_0+(V_{RF}/r)\times cos(\omega_{RF}t)+(\vec{E}_{THz}^{inc}\cdot\vec{l}_{eff}/r)\times cos(\omega_{THz}t+\varphi_{THz}) \quad (4)$$

The nonlinear electrical response of the photoconductor, arising from the slow electric field dependences of $v_{n,p}(E)$ and $\tau_{n,p}(E)$, leads to frequency components of the current density oscillating at angular frequencies $\omega\pm n\omega_{THz}\pm m\omega_{RF}$, with m, n integers. This mechanism can be exploited for multifrequency THz-wave generation or detection. The electrical response of the photoconductor is analytically calculated here by expressing the carrier densities and the current density as a power series expansion in terms of the amplitude of the oscillating field at a given bias electric field E_0.

Let's consider first the case of multifrequency generation with a photomixer operated with an optical beat in the THz domain, a radiofrequency electric field and no bias field. The amplitudes and phases of the spectral components of the current density in the photoconductor are calculated using numerical values from Table 1 and the results are displayed in Fig. 1.(a). The plot shows equidistant spectral components with slightly different phases. Two intense spectral components are situated, as expected, at angular frequencies $\omega \pm \omega_{RF}$. The phases and the amplitudes of the spectral components at $\omega+n\omega_{RF}$ and $\omega-n\omega_{RF}$ are the same. The dependences of the amplitudes and the phases of the spectral components with the amplitude of the oscillating electric field applied to the photoconductor are plotted in Fig. 1.(b). For fields up to a few 10^5 V/m, supralinear increases of the amplitudes are associated with stable values of the phases.

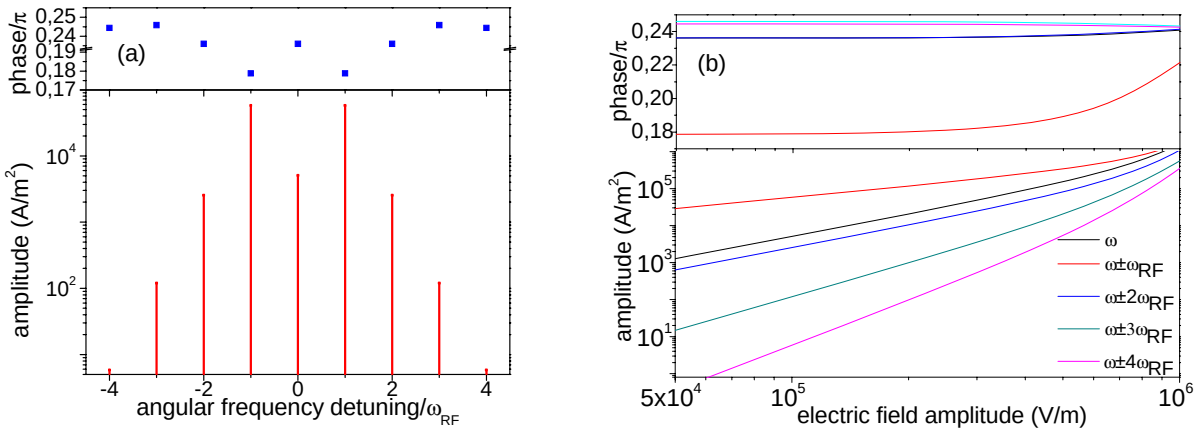

Figure 1. (a) Amplitude and phases of spectral components generated with an optical beat at $\omega=2\pi\times2$ THz and a radiofrequency modulation with amplitude $E_{RF}=10^5$ V/m at $\omega_{RF}=2\pi\times1$ MHz. The other parameters used for the calculations are taken from Table 1. (b) Dependences of amplitudes and phases in multifrequency generation in the photomixer with an alternative electric field.

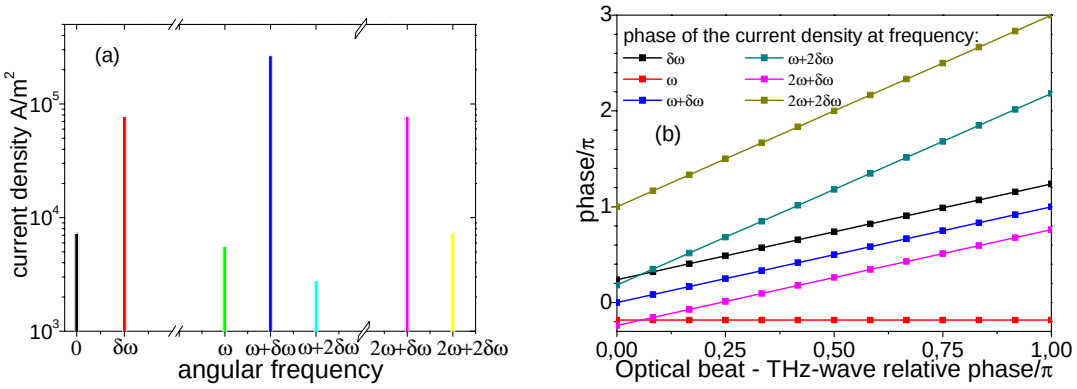

Figure 2.(a) Spectral components of the current density in the photomixer driven with an optical beat at $\omega=2\pi\times1$ THz and a THz-wave that induces an electric field with amplitude $E_{THz}=10^5$ V/m at $\omega+\delta\omega=2\pi\times1.001$ THz. The other parameters used for the calculations are taken from Table 1. (b) Dependences of the phases of the alternative components of the current density in the photomixer with the relative phase between the THz-wave and the optical beat.

Next, the photomixer operated with no bias field is used to detect a monochromatic THz-wave with an optical beat in the THz domain. The detuning between the optical beat and the THz-wave is in the microwave range. The spectral components of the current density are calculated using numerical values from Table 1 and the results are displayed in

Fig. 2.(a). The plot displays a dc current density, which corresponds to the rectified signal. There is a microwave spectral component at $\delta\omega=|\omega-\omega_{THz}|$ that correspond to the heterodyne detection signal. In addition, there are spectral components at angular frequencies of the THz-wave, optical beat and at mixing frequencies in the THz domain. Fig. 2.(b) displays a linear dependence of the phase of each alternative spectral component on the relative phase between the THz-wave and the optical beat.

3. EXPRIMENTAL RESULTS

The experimental setup (Fig. 3) is based on two extended cavity laser diodes emitting at 820 nm. Laser beams with the same power and linear polarisation are spatially superposed with a beamsplitter and focused with an aspheric lens on the photomixer active area. The photomixer is a 2 µm thick LTG-GaAs epitaxial layer grown on a semi-insulating GaAs substrate with a low-field electron recombination lifetime of 1.2 ps. A self-complementary log-spiral antenna with an outer radius of 1.5 mm drives the active area of 8 µm × 8 µm defined with interdigitated electrodes (1.8 µm gap, 0.2 µm width). The extremities of the antenna are connected with wire bonds to a semirigid 50-Ω microwave line addressed with a bias-T. On the DC port is coupled the bias voltage through a choke and, capacitively, the modulation signal from a low-frequency synthesizer (LF). The THz source is an active frequency multiplier (Militech AMC-10-R0000) driven by a microwave (MW) synthesizer. The output has mW-level power in the 75-110 GHz frequency range. The MW synthesizer can be additionally modulated with a radiofrequency synthesizer (RF). The optical beat can be modulated electrically by direct current modulation of a diode laser using a signal provided by RF_{LO} synthesizer. The photomixing signal is recorded with a microwave spectrum analyser with 50 Ω input impedance coupled on the AC port of the bias-T. The synthesizers and the spectrum analyser have an internal impedance of 50 Ω and are phase-referenced to the signal provided by a GPS-driven quartz oscillator with 10^{-12} level frequency accuracy.

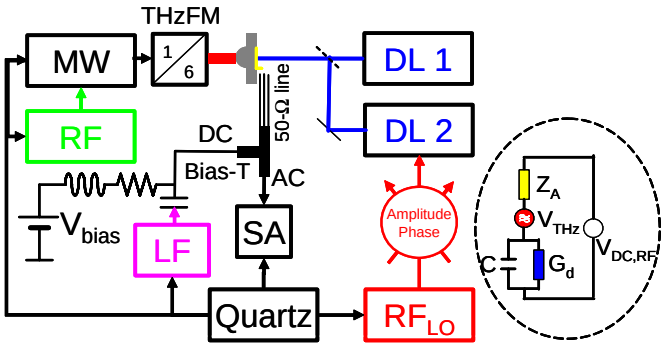

Figure 3. Experimental setup. DL1, DL2 diode lasers, SA spectrum analyzer, THzFM frequency multiplier. LF, RF, RF_{LO}, MW synthesizers referenced to a GPS-disciplined Quartz. Inset: equivalent model for the photomixer. Z_A antenna impedance, C electrodes capacitance, G_d optically-driven nonlinear photoconductance, V_{THz} antenna-induced Thévenin voltage, $V_{DC,RF}$ alternative voltage superposed on a continuous voltage.

Bifrequency operation of the photomixer driven by an optical beat in the microwave domain is observed by applying a low-frequency modulation signal. Fig. 4.(a) displays the spectrum of the photomixing signal. The spectral components with the highest amplitudes are at ~(1176±2) MHz with similar amplitudes. In addition, less intense spectral components at ~(1176±2×n) MHz for odd n are detected. The amplitudes of all spectral components are calculated with the numerical values from Table 1 and multiplied with a common factor in order to match the measured amplitudes of the two most intense spectral components. The calculated and experimental amplitudes of the spectral components at ~(1176±4) MHz agree. The model predicts also spectral components spaced by an even multiple of the modulation which are not experimentally detected.

A THz waveform is generated by frequency modulation of the MW synthesizer with a signal provided by the RF synthesizer. The spectrum of the THz waveform displays frequency components at $f_c \pm n f_{mod}$, centered on the carrier frequency f_c where n is an integer and f_{mod} is the modulation frequency, with amplitudes proportional to Bessel function

$J_n(\beta)$ of the modulation index β. This approach allows to generate a phase-coherent frequency comb in the THz domain with broadband tuning of the carrier frequency and of the modulation frequency by phase-referencing both synthesizers to a clock. A THz-wave at 89.52 GHz is down-converted in the microwave domain using the heterodyne detection and the recorded signal is shown in Fig. 4.(b.1). The responsivity of the heterodyne detection is at the 10^3 A/W level for the indicated experimental parameters. Next, the THz-wave is frequency-modulated at 2.5 MHz with a modulation index estimated at β~2.4. The heterodyne detection signal displays the frequency modulation sidebands, as shown in Fig. 4.(b.2). The bars, proportional with the corresponding Bessel functions, reproduce the measured amplitudes of the spectral components. Alternatively, the optical beat is modulated by direct current modulation with RF_{LO} of a laser diode at 2.5 MHz that generates THz frequency comb of photocurrents in the photoconductor. The amplitude of the modulating signal is adjusted in order to generate a frequency comb associated a β~2.4 frequency modulation index. The signal of heterodyne mixing with the THz-wave which is not modulated, shown in Fig. 4.(b.3), displays modulation sidebands. The amplitudes agree with the calculated values with the corresponding Bessel function which are plotted with bars.

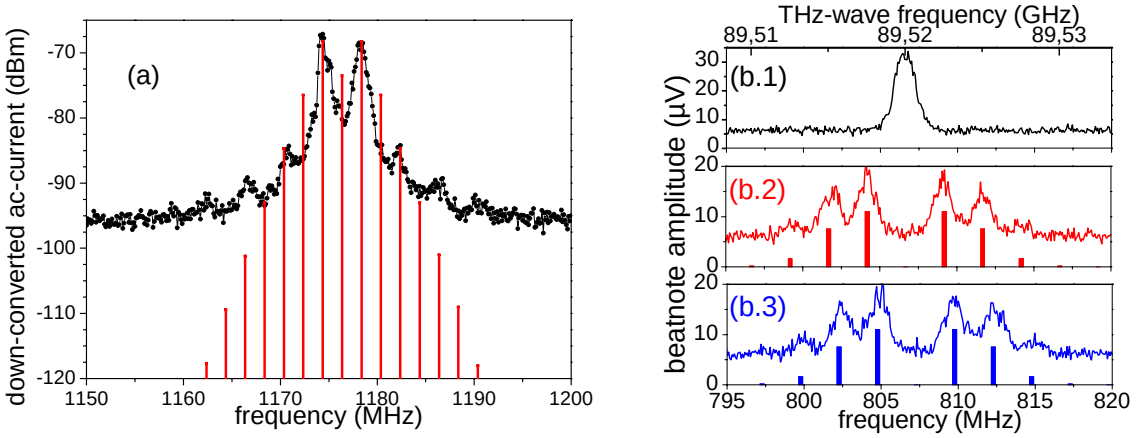

Figure 4.(a) Bifrequency operation of the photomixer in the microwave regime. Optical beat at $\omega=2\pi\times1176$ MHz, modulation at $\omega_m=2\pi\times2$ MHz, bias 4 mV, modulation amplitude 5 V at frequency 2 MHz. Combined optical power 2×20 mW. RBW 300 kHz, sweep time 4 ms, 16 video averages. The calculated amplitudes of the spectral components are plotted with red bars. (b.1) Heterodyne detection of a monochromatic THz-wave at 89.52 GHz. (b.2) Heterodyne detection signal for frequency modulation of the THz-wave. (b.3) Heterodyne detection signal for direct current modulation of a laser diode with an adjusted amplitude of RF_{LO}. The amplitudes of the spectral components, proportional with $J_n(\beta)$, are plotted with red bars. Frequency modulation at 2.5 MHz, modulation index $\beta=2.4$, combined optical beat power 2×20 mW. RBW=1 MHz, sweep time 5 ms, 10 video averages.

4. CONCLUSION

The generation and the detection of multifrequency THz-waves with a LTG-GaAs photomixer driven with the optical beat of two continuous-wave lasers are theoretically and experimentally demonstrated. The spectral components of the current density in the photoconductor are calculated in the case of the photomixing driven by an alternative electric field superposed to a bias electric field. Nonlinear electrical conduction mechanism is exploited for multifrequency generation in the microwave regime. THz waveforms are generated with a frequency multiplier driven by a microwave synthesizer that is modulated in the radiofrequency range. The optical beat, exploited as a local oscillator, provides down-conversion of the THz-waves to the microwave domain with the photomixer. This contribution demonstrates that the photomixing approach may be reconfigured easily for THz signal processing and may allow integration of local oscillator and mixer functions in a single photonic device.

REFERENCES

[1] S.S. Dhillon, et al., "The 2017 terahertz science and technology roadmap," J. Phys. D 50 (4), 043001 (2017).

[2] D. M. Mittleman, Sensing with THz Radiation, Springer-Verlag Berlin Heidelberg, 2003.

[3] E.R. Brown, K.A. McIntosh, K.B. Nichols, and C.L. Dennis, "Photomixing up to 3.8 THz in low-temperature-grown GaAs," Appl. Phys. Lett. 66 (3), 285–287 (1995).

[4] X. Yu, et al., "160 Gbit/s photonics wireless transmission in the 300-500 GHz band," APL Photonics 1 (8), 81301 (2016).

[5] T. Harter, et al., "Silicon-plasmonic integrated circuits for terahertz signal generation and coherent detection," Nature Photon. 12 (10), 625–633 (2018).

[6] F.L. Constantin, "Phase-coherent heterodyne detection in the terahertz regime with a photomixer," IEEE J. Quantum Electr. 47 (11), 1458–1462 (2011).

[7] N. Zamdmer, and Q. Hu, "Increase in response time of low-temperature-grown GaAs photoconductive switches at high voltage bias," Appl. Phys. Lett. 75 (15), 2313-2315 (1999).

[8] E.R. Brown, "A photoconductive model for superior GaAs THz photomixer," Appl. Phys. Lett. 75 (6), 769–771 (1999).

[9] E.R. Brown, K.A. McIntosh, F.W. Smith, K.B. Nichols, M.J. Manfra, C.L. Dennis, and J.P. Mattia, "Milliwatt output levels and superquadratic bias dependence in a low-temperature-grown GaAs photomixer," Appl. Phys. Lett. 64 (24), 3311–3313 (1994).